

Superconducting Splittable Quadrupole Magnet for Linear Accelerators

V.S. Kashikhin, N. Andreev, J. Kerby, Y. Orlov, N. Solyak, M. Tartaglia, G. Velev

Abstract—A new superconducting quadrupole magnet for linear accelerators was fabricated at Fermilab. The magnet is designed to work inside a cryomodule in the space between SCRF cavities. SCRF cavities must be installed inside a very clean room adding issues to the magnet design, and fabrication. The designed magnet has a splittable along the vertical plane configuration and could be installed outside of the clean room around the beam pipe previously connected to neighboring cavities. For more convenient assembly and replacement a “superferric” magnet configuration with four racetrack type coils was chosen. The magnet does not have a helium vessel and is conductively cooled from the cryomodule LHe supply pipe and a helium gas return pipe. The quadrupole generates 36 T integrated magnetic field gradient, has 600 mm effective length, and the peak gradient is 54 T/m. In this paper the quadrupole magnetic, mechanical, and thermal designs are presented, along with the magnet fabrication overview and first test results.

Index Terms—Linear Accelerator, Superconducting magnet, Quadrupole, Design, Fabrication, Test.

I. INTRODUCTION

SUPERCONDUCTING linear accelerators have a number of cryomodules with superconducting quadrupole magnets for beam focusing and steering. Various superconducting magnet designs were investigated for superconducting linacs [1]-[8]. These magnets were all bath cooled by LHe and should be assembled with superconducting RF (SCRF) cavities inside a clean room.

Akira Yamamoto, as the ILC [1] Project Manager, proposed to investigate for the 1.3 GHz cryomodule the version of splittable quadrupole. The magnet should be assembled around the beam pipe after all SCRF cavities are installed inside the clean room. In this case the magnet installation will be out of the clean room and will not contaminate the SCRF cavity inner surfaces.

The splittable quadrupole was designed and built at Fermilab, and tested in a 4.4 K helium bath at the FNAL Magnet Test Facility (MTF). We present the magnet specifications, design, main fabrication steps, the first test results on quench performance and measurements of the magnetic strength, field quality, and quadrupole center.

Manuscript received 12 September 2011.

V. S. Kashikhin, N. Andreev, J. Kerby, Y. Orlov, N. Solyak and M. Tartaglia, G. Velev are with the Fermi National Accelerator Laboratory, Batavia, IL 60510 USA (corresponding author phone: 630-840-2899; fax: 630-840-6766; e-mail: kash@fnal.gov).

II. QUADRUPOLE MAGNET DESIGN

The first FNAL unsplittable quadrupole magnet for ILC was tested in 2009 [5]. The main issue for the ILC quadrupole is to provide magnetic axis stability of several microns during a -20% focusing field change. This requirement arises from the Beam Based Alignment (BBA) technique, a procedure to determine the electron beam position relative to quadrupole magnetic center and adjust dipole correctors to move the beam on center. The magnetic and mechanical effects which correlate with magnetic axis stability must be eliminated.

A. Magnet Specification

The chosen quadrupole model parameters were close to those specified for the ILC Quadrupole [3] shown in Table 1.

TABLE I QUADRUPOLE SPECIFICATION

Parameter	Unit	Value
Integrated peak gradient	T	36
Aperture	mm	78
Effective length	mm	660
Peak gradient	T/m	54
Field non-linearity at 5 mm radius	%	0.05
Quadrupole strength adjustment for BBA	%	-20
Magnetic center stability at BBA	μm	5
Magnetic center offset in cryomodule	mm	0.3
Quadrupole azimuthal offset in cryomodule	mrad	0.3
Liquid helium temperature	K	2.2
Quantity required		560

B. Magnetic Design

In general the magnetic design for the quadrupole is very close to the previous model. During the first unsplittable model test [4] relatively strong coupling was observed between the quadrupole and dipole correctors wound on the top of quadrupole coils. This coupling through the superconductor magnetization [7]-[8] adds an extra value to the quadrupole magnetic center shift during strength variations. Also, because of yoke saturation effects the corrector transfer function is very non-linear, adding difficulty to the dipole corrector regulation. It was decided to separate the quadrupole and correctors to eliminate the cross talk

between magnets. Two shell type superconducting dipole correctors were built and successfully tested at FNAL [9].

TABLE II Quadrupole Model Parameters

Parameter	Unit	Value
Peak operating quadrupole current	A	100
Magnet total length	mm	680
SC wire diameter	mm	0.5
NbTi filament size (vendor value)	μm	3.7
Cu:SC volume ratio		1.5
Superconductor critical current at 5 T and 4.2 K	A	200
Coil maximum field at 100 A current	T	3.3
Magnetic field stored energy	kJ	40
Quadrupole inductance	H	3.9
Quadrupole coil number of turns/pole		900
Yoke outer diameter	mm	280

C. Mechanical Design and Fabrication

The quadrupole (see Fig. 1) has a vertical split plane and is assembled from two half cores (see Fig. 2) having racetrack superconducting coils on magnet poles.

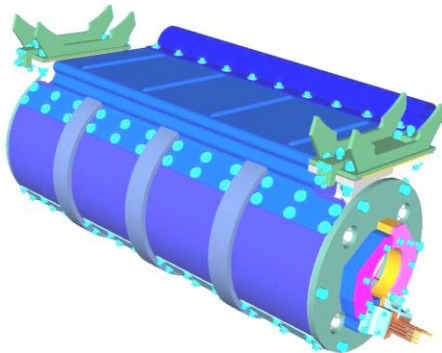


Fig. 1. The quadrupole magnet final assembly.

The magnet halves are tightened to each other by stainless steel bandage rings. This assembly is surrounded by Al thermal leads which have a good thermal contact with the cryomodule LHe supply line. The LHe line provides the cooling by conduction to this cryogen free magnet.

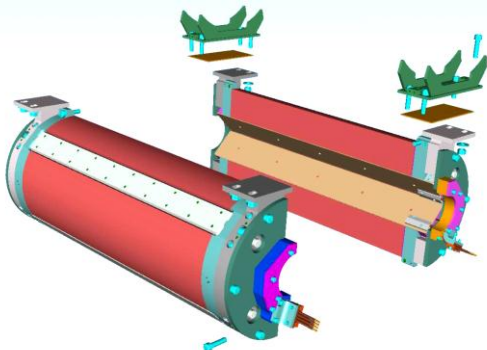


Fig. 2. View of the two quadrupole half cores split in the vertical plane.

The magnet core is assembled from 1.5 mm thick laser cut laminations fabricated from (Fermilab Main Injector) low carbon steel (see Fig. 3). The half core was pressed in a horizontal press and welded to sidebars and end plates forming a rigid mechanical structure. The magnet assembly is bolted to the support structure which is welded to the cryomodule 300 mm diameter helium return tube. Such position and connection eliminate the possible magnet motion during operation.

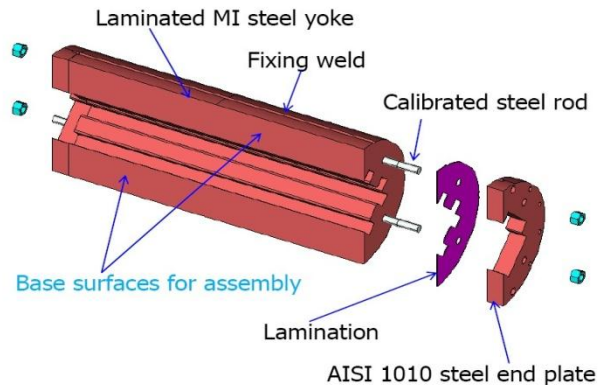


Fig. 3. The half core assembly.

The quadrupole has four racetrack type coils (see Fig. 4) each wound into an aluminum channel, with a stainless steel strip heater on top of each winding. This channel is used for the coil epoxy vacuum impregnation forming a closed mold. All heaters are connected in series and powered from the Test Stand heater firing unit when a quench is detected.



Fig. 4. Quadrupole racetrack coils in aluminum channel.

III. FIRST TEST RESULTS

The first tests were made in a 4.4 K bath-cooling mode at the MTF Stand 3 cryostat (see Fig. 5), in two thermal cycles.



Fig. 5. The quadrupole mounted to test stand top plate assembly.

Following the first cool down to 4.4 K, the magnet passed a hipot insulation standoff test of 500 V to ground, with leakage current of 0.2 μ A at 500V.

A. Quadrupole Training

The magnet load line and the superconductor critical current are shown in Fig. 5. The quadrupole operating current is well below the short sample current limit ~ 180 A. This provides a large temperature margin which is needed for the magnet operation in a conduction cooling mode.

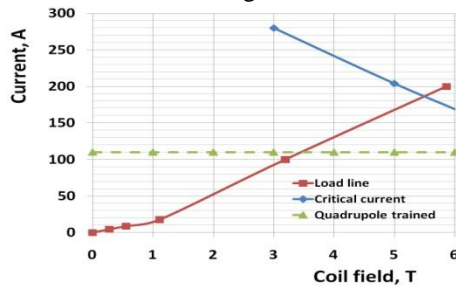


Fig. 5. Quadrupole load line and the short sample critical current.

The quench history is shown in Fig. 6 for the first thermal cycle. Training was generally at a steady rate of increasing quench current versus ramp number. Many of the events (shown in open symbols) were clearly fast voltage spikes that recovered, but were large enough to trigger the quench detection system (some up to 16 V across the coil, which resulted in a 5 V RC-filtered half coil difference signal). Very low (100 mV) initial quench detection thresholds were raised to 5 V to reduce trips due to transient spikes. Real quenches (filled symbols) were obvious with much slower voltage development; many true quenches clearly began with a voltage spike – perhaps the result of epoxy cracks or voids.

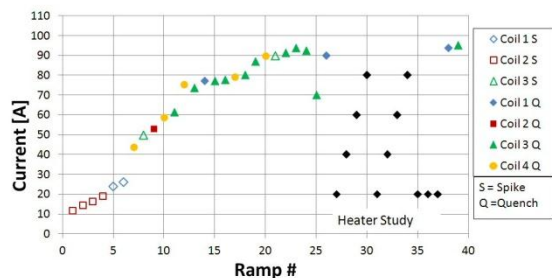


Fig. 6. The quadrupole quench history in first thermal cycle.

Spike and quench event locations moved around from coil to coil, although Coil 3 appears to be more prone to quenches than the others (see Fig. 7). The magnet was trained to 95 A in the time available for the first test. During the second thermal cycle the current exceeded the 100 A operating level (110 A is the upper limit due to helium venting capacity on the test stand). Fig. 7 summarizes the training curves for each coil in both thermal cycles.

It took several training quenches after the 110 A test stand current limit was reached before the magnet consistently reached and operated on a plateau at this current. After 30 minutes on the first plateau, the magnet quenched in coil 2; a

second plateau was then reached and operated for 40 minutes before it was necessary to end the test.

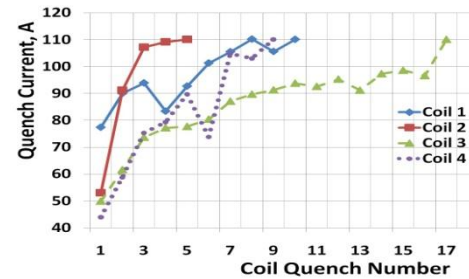


Fig. 7. Two thermal cycles quench training history for each quadrupole coil.

A typical voltage spike event is shown in Fig. 8, and a typical quench event is shown in Fig. 9.

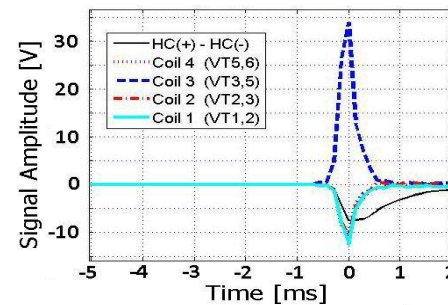


Fig. 8. Example of voltage spike signal (Coil 3) that recovered but still triggered the quench detection system (RC-filtered Half Coil signal).

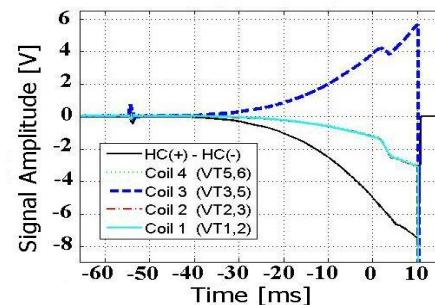


Fig. 9. A real quench in Coil 3 develops after a large voltage spike 55 ms before detection (at $t=0$).

B. Magnetic Measurements

For the first thermal cycle test program, magnetic measurements were made using a Senis 10 T 3D Hall probe calibrated with 0.1% linearity to 2 T. The Hall probe active element was approximately 8.0 mm radially out from the axis (though not precisely known, contributing some uncertainty to the calculated gradient). A calibrated 25 cm long, 25 mm diameter rotating tangential coil magnetic measurement system [10] was also used to measure body field strength and harmonics. At the specified 5 mm reference radius all measured harmonics were less than 2 units (.02 % of the quadrupole strength). This good field quality is explained by the large aspect ratio between the 39 mm pole tip radius and the 5 mm good field reference radius.

The measured magnetic field gradient is shown in Fig. 10. The 54 T/m gradient specified in Table 1 was reached at 90 A

current which provides 10 % margin relative to the 100 A peak design current.

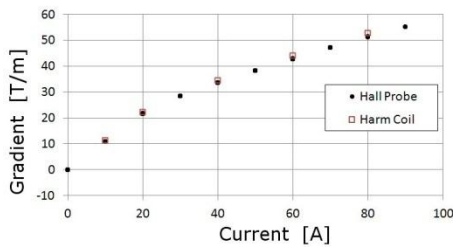


Fig. 10. The quadrupole gradient as function of current.

The body magnetic center stability was measured with BBA current profiles over a wide range of currents, up to 100 A (see Fig. 11). The center position was derived from the dipole field components assuming feed-down from the quadrupole [4], and could be measured reproducibly to $\sim 1 \mu\text{m}$ on each current plateau of several minutes duration. Center position dX (direction of the first normal quad pole) versus current is shown in Fig. 12 and Fig. 13 for the orthogonal direction dY .

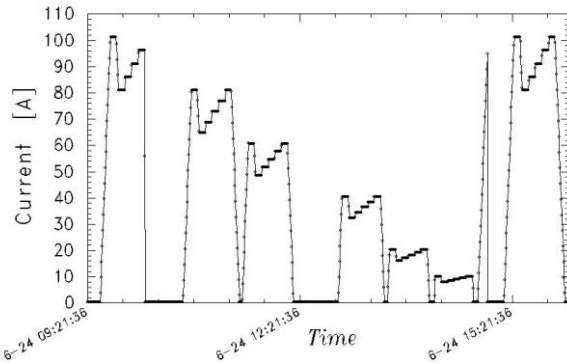


Fig. 11. BBA current profiles while measuring quadrupole center stability.

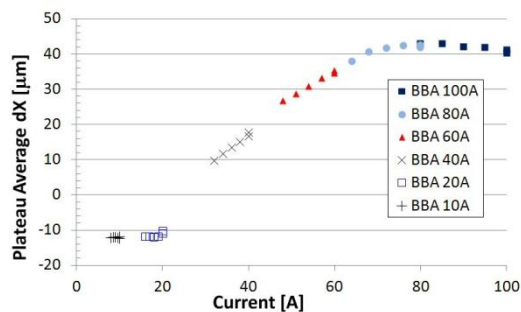


Fig. 12. X magnetic center position for current profiles of Fig.11.

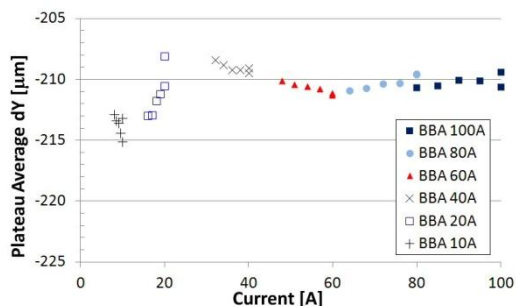


Fig. 13. Y magnetic center position for current profiles of Fig.11.

Fig. 14 summarizes the X and Y center position shifts due to the 20 % BBA gradient change at each nominal current. The measured behavior was quantitatively the same at two independent body positions, and slightly exceeds the specification in X at some currents. More careful control of the yoke gap size and uniformity may improve this.

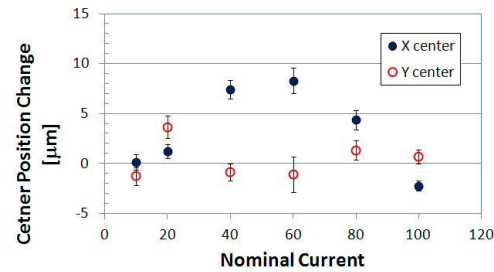


Fig. 14. Magnetic center shift as a function of operating current.

IV. CONCLUSION

The fabrication and test of a splittable quadrupole confirmed the design concept. After somewhat slow training, the magnet reached 20 % above the operational gradient. The quadrupole center position shift over a 20 % gradient change was close to, but slightly above, the desired level. Future plans are to improve the magnet split plane flatness to eliminate small gaps, and test again in a conduction-cooling mode.

ACKNOWLEDGMENT

Authors would like to thank A. Yamamoto, R. Kephart, M. Ross, and R. Stanek for useful discussions, and the possibility to work on this interesting and useful superconducting magnet technology project.

REFERENCES

- [1] "International Linear Collider Reference Design Report," <http://www.linearcollider.org/cms/?pid=1000025>.
- [2] "TESLA Design Report," Hamburg, DESY 2001-11, 2001.
- [3] V.S. Kashikhin *et al.*, "Design and Manufacturing Main Linac Superconducting Quadrupole for ILC at FERMILAB," *IEEE Transactions on Applied Superconductivity*, vol. 18, No. 2, June 2008, pp. 155-158.
- [4] V.S. Kashikhin, *et al.*, "Test results of a superconducting quadrupole model designed for linear accelerator applications," *IEEE Transactions on Applied Superconductivity*, vol. 19, Issue 3, Part 2, June 2009, pp. 1176-1182.
- [5] A. Koski, R. Bandelmann, S. Wolff, "Superconducting magnet package for the TESLA test facility," *IEEE Transactions on Magnetics*, vol. 32, No. 4, July 1996, pp. 2155-2158.
- [6] F. Toral *et al.*, "Design and fabrication study on the TESLA500 superconducting magnets," *IEEE Transactions on Applied Superconductivity*, vol. 12, No. 1, March 2002, pp. 282-286.
- [7] F. Toral, *et al.*, "Magnetization Effects on the Superconducting Combined Magnet Prototype for XFEL," *IEEE Transactions on Applied Superconductivity*, vol. 19, No. 3, June 2009, pp. 1136-1140.
- [8] C.M. Spencer, *et al.*, "Measuring the Magnetic Center Behavior and Field Quality of an ILC Superconducting Combined Quadrupole-Dipole Prototype," *IEEE Transactions on Applied Superconductivity*, vol. 20, Issue 3, May 2010, pp. 1964-1968.
- [9] V.S. Kashikhin, *et al.*, "Superconducting Magnets for SCRF Cryomodules at Front End of Linear Accelerators," Proceedings of IPAC'10, Kyoto, Japan, 2010, pp. 379-381.
- [10] G.V. Velev *et al.*, "A Fast Continuous Magnetic Field Measurement System Based on Digital Signal Processors," *IEEE Trans. of Applied Superconductivity*, Vol. 16, No. 2, June 2006, pp. 1374-1377.